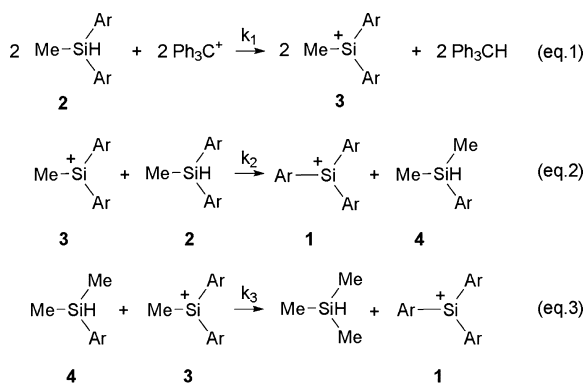
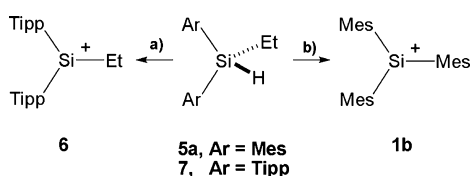




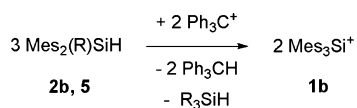
**Scheme 2. Suggested Reaction Course for the Formation of Triarylsilylium Ions 1 from Diarylmethylsilanes 2<sup>a</sup>**

**Scheme 3. BCS Hydride Transfer Reaction with Diaryl(ethyl)silanes 5a and 7<sup>a</sup>**


<sup>a</sup>(a) Ph<sub>3</sub>C<sup>+</sup>, rt, benzene, Ar = Tipp; (b) Ph<sub>3</sub>C<sup>+</sup>, rt, benzene, Ar = Mes.<sup>4</sup>

group, the size of the aryl substituent, and the nucleophilicity of the solvent on the reaction course. In addition we investigated the possible extension of this chemistry for the synthesis of triarylgermylum ions.

**RESULTS AND DISCUSSION**

Reaction of dimesitylalkylsilanes **2b** and **5a–c** with [Ph<sub>3</sub>C][B(C<sub>6</sub>F<sub>5</sub>)<sub>4</sub>] in benzene results in the formation of a biphasic mixture, which is typical for solutions of the [B(C<sub>6</sub>F<sub>5</sub>)<sub>4</sub>]<sup>−</sup> anion in aromatic hydrocarbons (Scheme 4). The more dense ionic

**Scheme 4. BCS Hydride Transfer Reaction with Dimesitylsilanes 2b and 5a–d<sup>a</sup>**


<sup>a</sup>**2b**: R = Me, **5a**: R = Et; **5b**: R = *i*-Pr; **5c**: R = *t*-Bu; **5d**: R = SiMe<sub>3</sub>.

phase contains the trimesitylsilylium borate **1b**[B(C<sub>6</sub>F<sub>5</sub>)<sub>4</sub>], and the corresponding neutral trialkylsilane is detected in the lighter phase. In each case the silylium ion **1b** was identified by multinuclear NMR spectroscopy. Particularly useful for this purpose was its characteristic low-field <sup>29</sup>Si NMR chemical shift at δ<sup>29</sup>Si = 225.3 (see Table 1 and Figure S10, Supporting Information (SI)). In case of dimesityl-*tert*-butylsilane, **5c**, the hydride abstraction appears to be very slow, probably due to the high steric demand. In this case even after 24 h of stirring at room temperature with excess silane (**5c**: [Ph<sub>3</sub>C][B(C<sub>6</sub>F<sub>5</sub>)<sub>4</sub>] = 2:1), major amounts of trityl cation were detected in the mixture by NMR spectroscopy. A signal at δ<sup>29</sup>Si = 225.3 was however observed, indicating the formation of Mes<sub>3</sub>Si<sup>+</sup>, **1b** (Figure S10d). The reaction time was not extended to completeness of the reaction, since prolonged stirring at room temperature resulted in slow decomposition of cation **1b**.

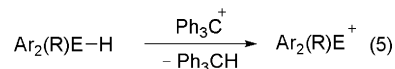
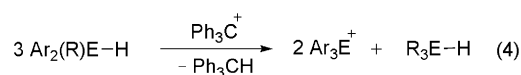
In contrast to the clean reactions observed in the cases of the alkylsilanes **2b**, **5a,b**, the reaction of disilane **5d** with trityl cation led only to a complicated mixture of products, both at room temperature and at −10 °C. Although <sup>1</sup>H and <sup>13</sup>C NMR spectroscopy of the product mixture indicated the formation of triphenylmethane, Ph<sub>3</sub>CH, <sup>29</sup>Si NMR spectroscopy provided no indication for the formation of silylium ion **1b** in this case.

Steric protection of the incipient diaryl(methyl)silylium ion **3**, formed in the first reaction step (Scheme 2) by the aryl substituent, is mandatory for the reaction to occur. Therefore, a series of diarylmethyl silanes **2** substituted with bulky aryl groups yields the corresponding triarylsilylium ions **1** upon treatment with trityl cation (Scheme 1). This is demonstrated in each case by the low-field <sup>29</sup>Si NMR resonance detected for silylium borates **1**[B(C<sub>6</sub>F<sub>5</sub>)<sub>4</sub>] in the region of δ<sup>29</sup>Si = 216.2–229.9 (see Table 1). The low-field position of the <sup>29</sup>Si resonance is for most of the silylium ions independent of the solvent as long as arenes are used (see Table 1). The largest steric effect was detected for Tipp<sub>2</sub>EtSi<sup>+</sup>, **6**, for which a slightly more shielded <sup>29</sup>Si NMR signal was found in chlorobenzene[D<sub>5</sub>] than in benzene[D<sub>6</sub>] (Δδ<sup>29</sup>Si = −4.1, see Table 1).

Interestingly, dixylyl-substituted silane **2a** cleanly underwent the substituent exchange to give silylium ion Xylyl<sub>3</sub>Si<sup>+</sup>, **1a**, while di-*ortho*-tolylmethyl silane, *o*-Tol<sub>2</sub>MeSiH, **2f** (and likewise diphenylmethylsilane, Ph<sub>2</sub>MeSiH, **2g**, or mesityldimethylsilane, MesMe<sub>2</sub>SiH, **9**), failed to give the corresponding silylium ion. <sup>29</sup>Si NMR signals in the range typical for silylated arenium ions (δ<sup>29</sup>Si = 80–100) indicated in these cases the formation of benzenium ions **8** (Scheme 5).<sup>9b,11</sup> These results suggest that the formation of relatively stable arenium ions in the case of the reaction of the sterically less hindered silanes **2f,g** with trityl cation inhibits the intermolecular substituent exchange. This is further supported by the results of quantum mechanical computations,<sup>12,13</sup> which indicate that for silylium ion Xylyl<sub>2</sub>MeSi<sup>+</sup>, **3a**, produced in the first step of the reaction sequence leading to cation **1a** (Scheme 2) complexation with benzene is an endergonic process at room temperature (ΔG<sup>298</sup> = +8 kJ mol<sup>−1</sup>), while for the related silylium ion *o*-Tol<sub>2</sub>MeSi<sup>+</sup>, **3f**, benzenium ion formation is thermodynamically favored (ΔG<sup>298</sup> = −30 kJ mol<sup>−1</sup>, all values computed at M05-2X/6-311+G(d,p)). The significantly different Si–C separations in the computed molecular gas phase structures of benzenium ions **8f** and in the solvent complex **1a**/benzene reflect their different thermodynamic stability at room temperature (see Figure 1).

As a consequence, the formation of stable solvent complexes is expected to hamper the intermolecular substituent exchange reaction also for more bulky substituted diarylsilylium ions **3**. To verify this conclusion, the reaction of dimesitylmethylsilane **2b** with trityl cation was conducted in the significantly stronger donor solvent acetonitrile. In this case exclusively the dimesitylmethylsilyl nitrilium ion **10** was formed, establishing that the substituent exchange is inhibited by the formation of strong silylium ion/solvent complexes. The silylnitrilium ion **10** was identified by its high-field <sup>29</sup>Si NMR resonance (δ<sup>29</sup>Si = 10.6), which appears at somewhat higher field than those reported for related trialkylsilylnitrilium ions.<sup>1c,14</sup> The structural integrity of the dimesitylmethylsilyl unit is demonstrated by the <sup>1</sup>H/<sup>29</sup>Si-HMBC NMR spectrum, which shows a cross signal for the resonances of the methyl protons and the <sup>29</sup>Si nuclei (Figure 2).

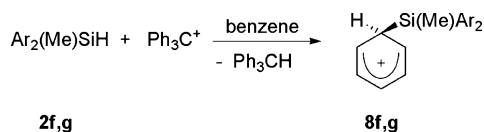
**Table 1. Products from the BCS Hydride Transfer Reaction between Trityl Cation and Different Silanes and Germanes According to Eqs 4 and 5 along with Characteristic  $^{29}\text{Si}$  NMR Chemical Shifts for Formed Silyl Cations**



starting silane	Ar	R	E	reaction according to equation	cation	$\delta^{29}\text{Si}$ (cation)	solvent	ref
2a	Xylyl	Me	Si	4	1a	229.9	$\text{C}_6\text{D}_6$	4
2b	Mes	Me	Si	4	1b	225.3	$\text{C}_6\text{D}_6$	4, 7
2b	Mes	Me	Si	5	10 <sup>a</sup>	10.6	$\text{C}_6\text{D}_6/\text{CH}_3\text{CN}$	this work
2c	Duryl	Me	Si	4	1c	226.5	$\text{C}_6\text{D}_6$	this work, <sup>e</sup> 7
2d	Pemp	Me	Si	4	1d	216.2	$\text{C}_6\text{D}_6$	4
						216.4	$\text{C}_7\text{D}_8$	this work
						216.8	$\text{C}_6\text{D}_5\text{Cl}$	this work
2e	Tipp	Me	Si	4	1e	229.8	$\text{C}_6\text{D}_6$	4
2f	<i>o</i> -Tol	Me	Si	5	8f <sup>b</sup>		$\text{C}_6\text{D}_6$	this work
2g	Ph	Me	Si	5	8g <sup>b</sup>		$\text{C}_6\text{D}_6$	this work
5a	Mes	Et	Si	4	1b	225.3	$\text{C}_6\text{D}_6$	4 <sup>e</sup>
5b	Mes	<i>i</i> -Pr	Si	4	1b	225.3	$\text{C}_6\text{D}_6$	this work <sup>e</sup>
5c	Mes	<i>t</i> -Bu	Si	4	1b <sup>c</sup>	225.3	$\text{C}_6\text{D}_6$	this work <sup>e</sup>
5d	Mes	$\text{SiMe}_3$	Si		<sup>d</sup>		$\text{C}_6\text{D}_6$	this work
7	Tipp	Et	Si	5	6	244.7	$\text{C}_6\text{D}_6$	4
						240.6	$\text{C}_6\text{D}_5\text{Cl}$	this work
11a	Mes	Me	Ge	4	12a		$\text{C}_6\text{D}_6$	this work <sup>e</sup>
11b	Tipp	Me	Ge	5	13		$\text{C}_6\text{D}_6$	this work <sup>e</sup>

<sup>a</sup>No substituent exchange occurred. <sup>b</sup>More than one signal was observed in the  $^{29}\text{Si}$  NMR spectra, but no triarylsilyl cation could be detected. <sup>c</sup>Only minor conversion of silane after 24 h, due to the high steric demand. <sup>d</sup>Product mixture obtained. <sup>e</sup>See also the SI.

**Scheme 5. BCS Hydride Transfer Reaction of Diaryl(methyl)silanes 2f,g with trityl cation<sup>a</sup>**



<sup>a</sup>f: Ar = 2-methylphenyl (*o*-Tol); g: Ar = phenyl (Ph).

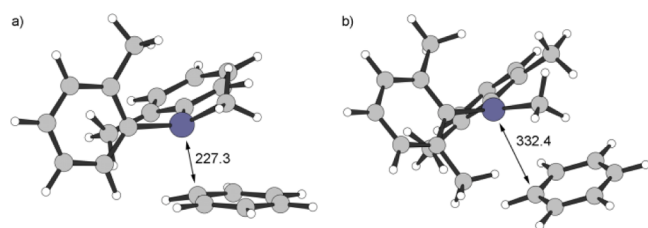


**Figure 1.** Calculated molecular structures for complexes (a) [*o*-Tol<sub>2</sub>MeSi<sup>+</sup>/C<sub>6</sub>H<sub>6</sub>] (8f) and (b) [Xylyl<sub>2</sub>MeSi<sup>+</sup>/C<sub>6</sub>H<sub>6</sub>] at the M05-2X/6-311+G(d,p) level of theory. Atomic distances are given in pm.

The possible extension of the investigated intermolecular substituent exchange reaction on diarylmethylgermanes was tested for the dimesitylmethyl-, Mes<sub>2</sub>MeGeH, 11a, and bis(triisopropylphenyl)methylgermane, Tipp<sub>2</sub>MeGeH, 11b. Both germanes gave with [Ph<sub>3</sub>C][B(C<sub>6</sub>F<sub>5</sub>)<sub>4</sub>] biphasic reaction mixtures in benzene. In the case of mesitylgermane 11a <sup>1</sup>H and <sup>13</sup>C NMR spectroscopy of the lower ionic phase showed the clean formation of trimesitylgermylium borate, 12a[B(C<sub>6</sub>F<sub>5</sub>)<sub>4</sub>] (see Figures S4, S5, SI).<sup>15</sup> This borate had been synthesized previously by the Lambert group,<sup>7b</sup> and the comparison revealed an almost perfect match of the <sup>1</sup>H and <sup>13</sup>C NMR

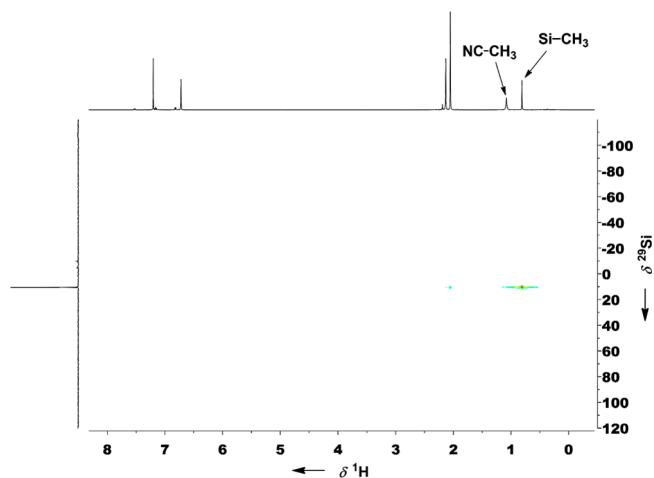
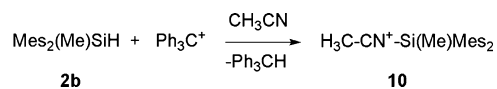


**Figure 2.** <sup>1</sup>H, <sup>29</sup>Si-HMBC NMR spectrum of 10[B(C<sub>6</sub>F<sub>5</sub>)<sub>4</sub>] (499.87 MHz/99.31 MHz, 305 K, C<sub>6</sub>D<sub>6</sub>).

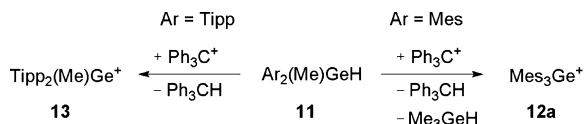
**Scheme 6. Formation of Dimesitylmethylsilyl Nitrium Ion 10 from Dimesityl(methyl)silane 2b**



data. The side product in the substituent exchange reaction, Me<sub>3</sub>GeH, was detected in the nonpolar phase by GC-MS analysis. Further support for the identification of Mes<sub>3</sub>Ge<sup>+</sup>, 12a, came from its derivatization reaction with tributyltin and the subsequent detection of trimesitylgermane, Mes<sub>3</sub>GeH, by GC-MS analysis. The attempted synthesis of Tipp<sub>3</sub>Ge<sup>+</sup>, 12b, under the same reaction conditions however failed. Instead, reaction

of  $\text{Tipp}_2\text{MeGeH}$ , **11b**, with  $[\text{Ph}_3\text{C}][\text{B}(\text{C}_6\text{F}_5)_4]$  yielded the regular hydride transfer product bis(triisopropylphenyl)methylgermylium, **13**, without rearrangement (Scheme 7). The

### Scheme 7. BCS Hydride Transfer Reaction of Germanes **11**<sup>a</sup> with Trityl Cation

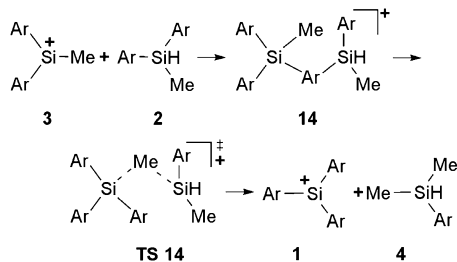


<sup>a</sup>a: Ar = 2,4,6-trimethylphenyl (Mes); b: Ar = 2,4,6-triisopropylphenyl (Tipp).

identity of cation **13** was confirmed by  $^1\text{H}$  and  $^{13}\text{C}$  NMR spectroscopy.<sup>13</sup> Two-dimensional NMR spectroscopy was particularly important for the structure elucidation. Decisive for the identification of the TippGeMe linkage in cation **13** was the detection of cross-signals in the  $^1\text{H}$ ,  $^{13}\text{C}$ -HMBC between the methyl hydrogen atoms and the *ipso*-carbon atoms of the Tipp substituent (see Figure S8a,b, SI). Additional support came from  $^1\text{H}$ ,  $^1\text{H}$ -NOESY spectroscopy, which revealed a close spatial relation between the isopropyl groups of the aryl substituent and the methyl group at germanium (see Figure S9, SI) This behavior of germane  $\text{Tipp}_2(\text{Me})\text{GeH}$ , **11b**, in the BCS hydride transfer reaction, which is remarkably different from that of silane  $\text{Tipp}_2(\text{Me})\text{SiH}$ , **2e**, emphasizes that the intermolecular substituent exchange as observed in the case of the silane crucially depends on subtle steric and electronic effects.

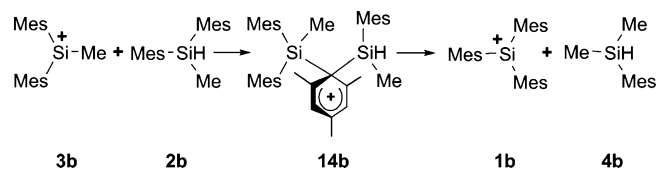
The general reaction course of the substituent exchange reaction as shown in Scheme 2 is supported by cross experiments, by the applied stoichiometry, and by the identification of the byproducts as outlined in a previous communication.<sup>4</sup> The actual mechanism of the key step, the intermolecular aryl/methyl exchange between the diarylmethylsilylium ion **3** and the corresponding silane **2** is however less clear (Scheme 8). With respect to similar intramolecular

### Scheme 8. Proposed Reaction Mechanism for the Intermolecular Alkyl–Aryl Exchange



substituent exchange reactions studied earlier in our group,<sup>3g</sup> we suggested arenium ions **14** as possible intermediates, which transform via a methonium-like transition state into the products.<sup>4</sup> The results of preliminary calculations at the M06-2X/6-311G(d,p) level of theory support this view.<sup>12,13</sup> The formation of trimesitylsilylium **1b** by reaction of silylium ion **3b** with silane **2b** is predicted to be exergonic at ambient temperature by  $\Delta G^{298} = -40.5 \text{ kJ mol}^{-1}$ , and also the formation of intermediate **14b** from the reactants is slightly exergonic ( $\Delta G^{298} = -8.3 \text{ kJ mol}^{-1}$ , Scheme 9).

### Scheme 9. Intermolecular Mesityl/Methyl Transfer to Give Trimesitylsilylium **1b** via the Mesitylenium Cation **14b**



Tri- and diaryl tetrylium borates  $[\text{Ar}_3\text{E}][\text{B}(\text{C}_6\text{F}_5)_4]$  and  $[\text{Ar}_2\text{RE}][\text{B}(\text{C}_6\text{F}_5)_4]$  (E = Si, Ge) are stable in the solid state at room temperature. In arene solution slow decomposition occurs even at  $-10^\circ\text{C}$ , in particular in the case of sterically less hindered cations such as **1a,b**.<sup>4</sup> The decomposition is significantly slower for highly substituted cations such as tris(pentamethylphenyl)silylium,  $\text{Pemp}_3\text{Si}^+$ , **1d**. While for the less bulky substituted cations all attempts to grow crystals suitable for X-ray diffraction (XRD) analysis resulted in crystals of decomposition products,<sup>4</sup> crystallization of a salt of cation **1d** was achieved by replacing the tetrakis(pentafluorophenyl)-borate anion by the dodecachloro-*closo*-dodecaborate dianion  $[\text{B}_{12}\text{Cl}_{12}]^{2-}$ . Recent work from the Knapp, Reed, Ozerov, and Oestreich laboratories revealed the superior crystallization ability of this robust, weakly coordinating anion.<sup>16</sup> Crystals suitable for XRD analysis were obtained from an *ortho*-dichlorobenzene solution of  $[\text{Pemp}_3\text{Si}]_2[\text{B}_{12}\text{Cl}_{12}]$  at  $-15^\circ\text{C}$  after four weeks.<sup>13</sup> The asymmetric unit contains one cation, three *ortho*-dichlorobenzene molecules, and one-half of the anion. The crystal structure solution indicates some positional disorder of one of the solvent molecules, which was resolved by using a split model with a 5:2 occupation. The crystal structure of the salt reveals well-separated cations, anions, and solvent molecules (Figure 3). In particular, no chlorine atom of the *closo*-borate dianion or solvent molecules approaches the silicon atom at a distance smaller than 489 pm. Silylium ion **1d** adopts the propeller-shaped conformation that is typical for triaryl-substituted compounds of the general  $\text{AB}_3$  composition. The trigonal planar coordination environment for the silicon atom is indicated by the summation of all bond angles  $\alpha$  around the silicon atom to  $360.0^\circ$  (Figure 4a).  $\text{Si}-\text{C}^{\text{ipso}}$  bond lengths in  $\text{Pemp}_3\text{Si}^+$  (average  $\text{Si}-\text{C}^{\text{ipso}}$ : 184.72(57) pm) are slightly longer than found for  $\text{Mes}_3\text{Si}^+$  in the crystal structure of  $[\text{Mes}_3\text{Si}][\text{HCB}_{11}\text{Me}_5\text{Br}_6]$  (181.7 pm).<sup>7c</sup> Also the dihedral angles  $\beta$  between the central  $\text{C}^{\text{ipso}}\text{Si}^+$  plane and the plane of the aryl rings of the substituents ( $\beta = 51.4\text{--}65.1^\circ$ , average value of  $\beta = 60.0^\circ$ , see Figure 4b) are larger than reported for  $\text{Mes}_3\text{Si}^+$  (average  $\beta = 49.2^\circ$ ).<sup>7c</sup> Both structural differences between the closely related cations **1b** and **1d** can be attributed to the somewhat larger steric effects of the Pemp substituent due to the buttressing influence of the *meta* and *para* methyl groups. On the other hand, the average  $\text{Si}-\text{C}^{\text{ipso}}$  bond in cation **1d** is significantly shorter than found experimentally for the tetracoordinated silanes tris(pentamethylphenyl)silane,  $\text{Pemp}_3\text{SiH}$  (194.96(42) pm),<sup>4</sup> and bis(pentamethylphenyl)methylsilane,  $\text{Pemp}_2(\text{Me})\text{SiH}$ , **2d** (190.18(32) pm).<sup>13</sup> This bond length shortening results from the superposition of two effects. The reduced steric congestion in the trigonal planar coordinated cation **1d** compared to the tetrahedral silanes allows for shorter  $\text{Si}-\text{C}^{\text{ipso}}$  bonds. In addition, the smaller covalent radii of tricoordinated silicon and the onset of  $\pi$ -conjugation between the Pemp substituent and the central silicon atom contribute to the shorter  $\text{Si}-\text{C}^{\text{ipso}}$  bond in silylium ion **1d** in particular in comparison with the diaryl-substituted

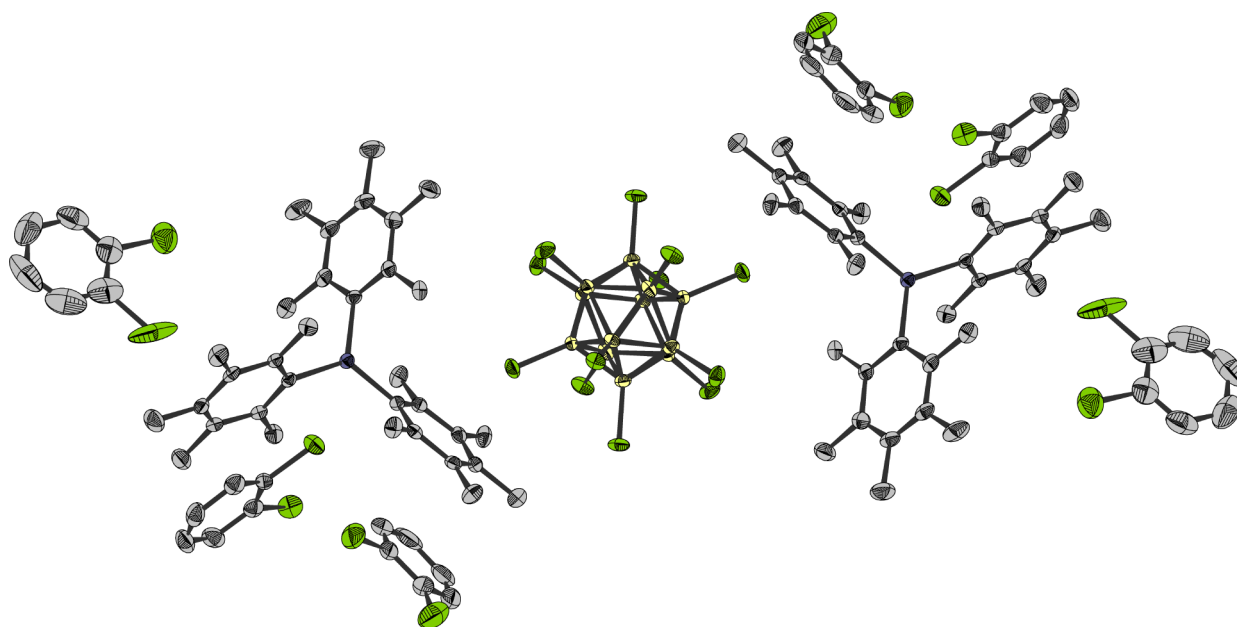


**Figure 3.** Ellipsoid presentation of the double asymmetric unit of  $[\text{Pemp}_3\text{Si}]_2[\text{B}_{12}\text{Cl}_{12}] \cdot 6 \text{ } o\text{-Cl}_2\text{C}_6\text{H}_4$  in the crystal (H atoms omitted for clarity; thermal ellipsoids at 50% probability level). Color code: gray, carbon; blue, silicon; yellow, boron; green, chlorine.

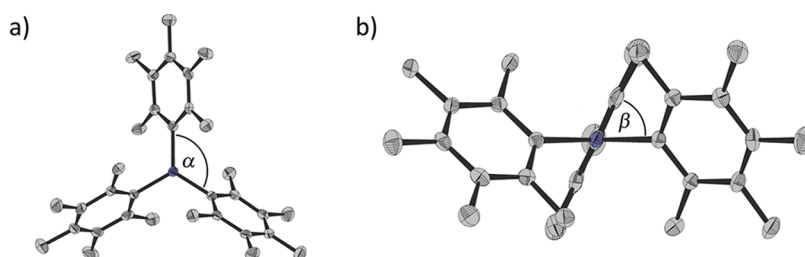


**Figure 4.** Ellipsoid presentation of the molecular structure of  $\text{Pemp}_3\text{Si}^+$ , **1d**, in the crystal: (a) view perpendicular to the  $\text{SiC}^{ipso}_3$  plane; (b) view along one  $\text{Si}-\text{C}^{ipso}$  vector (H atoms omitted for clarity; thermal ellipsoids at 50% probability level). Color code: gray, carbon; blue, silicon. Pertinent angles [deg] and bond lengths [pm]:  $\text{Si}-\text{C}^{ipso}$ : 184.2(6), 184.5(4), 185.5(4);  $\text{C}^{ipso}-\text{C}^{ortho}$  (av): 140.47(72);  $\text{C}^{ortho}-\text{C}^{meta}$  (av): 140.18(80);  $\text{C}^{meta}-\text{C}^{para}$  (av): 139.81(79);  $\alpha$ : 117.9(2), 119.7(2), 122.4(2);  $\beta$ : 51.4(5), 63.5(2), 65.1(2).

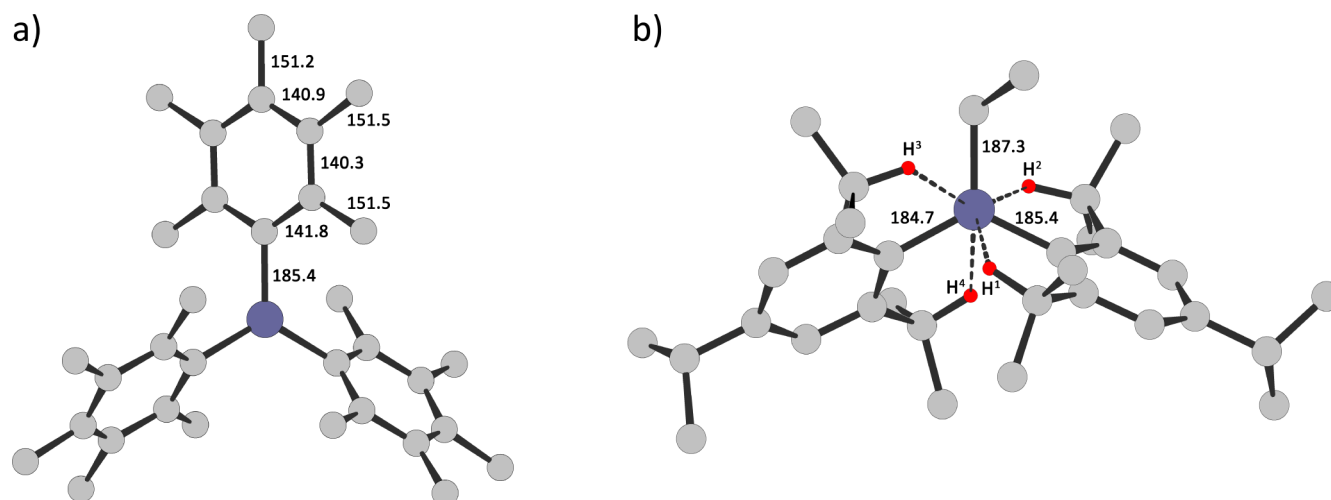


**Figure 5.** Calculated molecular structure of silylium ions at B3LYP/6-311G(d,p) (pertinent bond lengths and interatomic distances are given [pm]; all H atoms except methine H atoms are omitted for clarity. Color code: gray, carbon; blue, silicon; red, hydrogen). (a)  $\text{Pemp}_3\text{Si}^+$ , **1d** ( $\text{C}_3$  molecular symmetry); (b)  $\text{Tipp}_2\text{EtSi}^+$ , **6**. ( $\text{Si}-\text{H}^1$ : 238.2,  $\text{Si}-\text{H}^2$ : 256.5,  $\text{Si}-\text{H}^3$ : 252.0,  $\text{Si}-\text{H}^4$ : 255.8).

silane **2d**. DFT computations at the B3LYP/6-311G(d,p) level of theory predict a structure of molecular  $\text{C}_3$  symmetry for  $\text{Pemp}_3\text{Si}^+$ , **1d**, which is very close to the experimentally

determined structure in all relevant parameters (see Figure 5a). A major difference between the molecular structures derived from XRD and from DFT calculations<sup>12,13</sup> can be found for the

dihedral angle  $\beta$ , which is computed to be  $51.8^\circ$ ,  $8.2^\circ$  smaller than the average value in the experimental structure. Accordingly,  $^{29}\text{Si}$  NMR chemical shift calculations based on this molecular structure resulted in a predicted isotropic  $^{29}\text{Si}$  NMR chemical shift for silylium ion **1d** of  $\delta^{29}\text{Si}^{\text{calc}} = 221.6$  (Table 2), in good agreement with the NMR chemical shift found in solution.

**Table 2.**  $^{29}\text{Si}$  NMR Chemical Shift Data of Silylium Ion **1d** in Solution and in the Solid State and Its Experimental and Calculated<sup>a</sup> (*italic*)  $^{29}\text{Si}$  NMR Chemical Shift Tensor

Pemp <sub>3</sub> Si <sup>+</sup> , <b>1d</b>	$\delta_{\text{iso}}^b$	$\delta_{11}$	$\delta_{22}$	$\delta_{33}$	$\Omega^c$	$\kappa^d$
C <sub>6</sub> D <sub>6</sub>	216.2					
solid state	223.5	329	312	30	299	0.89
calculated <sup>a</sup>	221.6	320	318	27	293	0.99

<sup>a</sup>Calculated at GIAO/B3LYP/IGLOIII//B3LYP/6-311G(d,p). <sup>b</sup> $\delta_{\text{iso}} = 1/3(\delta_{11} + \delta_{22} + \delta_{33})$ . <sup>c</sup>Span  $\Omega = \delta_{11} - \delta_{33}$ . <sup>d</sup>Skew  $\kappa = 3(\delta_{22} - \delta_{\text{iso}})/\Omega$ .

The measured  $^{29}\text{Si}$  NMR chemical shift of **1d**[B(C<sub>6</sub>F<sub>5</sub>)<sub>4</sub>] is insensitive to changes of the arene solvent (see Table 1). CPMAS solid-state NMR spectroscopy (see Figure 6) showed a

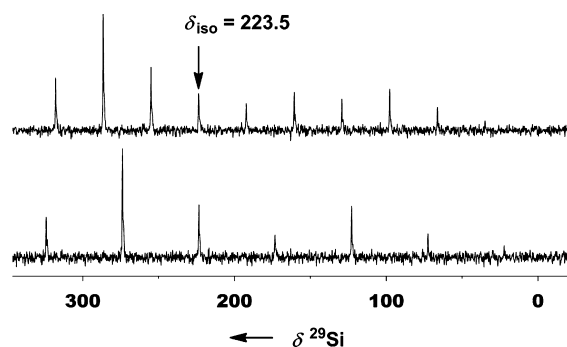


**Figure 6.**  $^{29}\text{Si}$  CPMAS NMR spectra of [Pemp<sub>3</sub>Si]<sub>2</sub>[B<sub>12</sub>Cl<sub>12</sub>]·6 o-Cl<sub>2</sub>C<sub>6</sub>H<sub>4</sub> at 4 kHz rotation frequency (lower trace) and at 2.5 kHz (upper trace).

slightly more deshielded  $^{29}\text{Si}$  resonance for the salt **1d**<sub>2</sub>[B<sub>12</sub>Cl<sub>12</sub>] ( $\delta_{\text{iso}}^{29}\text{Si} = 223.5$ ). Analysis of the slow spinning  $^{29}\text{Si}$  CPMAS NMR spectra revealed within the limits of accuracy (standard deviation for the principal components: 3 ppm) an almost oblate  $^{29}\text{Si}$  NMR chemical shift tensor ( $\delta_{11} = \delta_{22} > \delta_{33}$  and skew  $\kappa$  close to +1) in agreement with the axial molecular symmetry of silylium ion **1d** (see Table 2).<sup>13,17,18</sup> The high anisotropy of the  $^{29}\text{Si}$  NMR chemical shift tensor is indicated by its large span  $\Omega = \delta_{11} - \delta_{33} = 299$ . A similar highly anisotropic chemical shift tensor of axial symmetry was determined for [Mes<sub>3</sub>Si][HCB<sub>11</sub>Me<sub>5</sub>Br<sub>6</sub>].<sup>7c</sup> Therefore, the anisotropy of the  $^{29}\text{Si}$  chemical shift tensor is significantly larger for triarylsilylium ions than for tetrahedral-coordinated silicon compounds (i.e., for triphenylsilane, Ph<sub>3</sub>SiH,  $\Omega = 52$ ).<sup>19</sup> In fact, the spans  $\Omega$  for triaryl silylium ions approach those determined for disilenes ( $\Omega = 161\text{--}514$ )<sup>20</sup> but are still somewhat smaller than measured for N-heterocyclic silylenes ( $\Omega = 328\text{--}376$ ).<sup>21</sup>

The origin of this high anisotropy of the  $^{29}\text{Si}$  NMR chemical shift tensor of silylium ion **1d** is the strongly deshielded  $\delta_{11}$  and  $\delta_{22}$  components ( $\delta_{11} = 329$ ;  $\delta_{22} = 312$ ), while the high-field component  $\delta_{33}$  is in the chemical shift range for tetracoordinated silicon atoms ( $\delta_{33} = +30$  to  $-60$ ; see also Table 2).<sup>19</sup> For symmetry reasons both deshielded principal components are

located in the SiC<sup>ipso</sup><sub>3</sub> plane of **1d**, and the shielded component  $\delta_{33}$  is oriented perpendicular to that plane and along the local C<sub>3</sub> axis (see Figure 7). This orientation of the  $^{29}\text{Si}$  NMR



**Figure 7.** Orientation of the principal axes of the  $^{29}\text{Si}$  NMR chemical shift tensor in silylium ion **1d**.

chemical shift tensor relative to the molecular structure and also the size of the principal components are confirmed by the results of NMR chemical shift computations (see Table 2). A more detailed analysis<sup>22,23</sup> of the calculations suggests that the strong deshielding of the in-plane components  $\delta_{11}$  and  $\delta_{22}$  is mainly the result of paramagnetic currents induced by the magnetic field that correlates the degenerate Si–C  $\sigma$ -bonding orbitals with the LUMO, which is dominated by contributions from the 3p(Si). These deshielding currents are very efficient due to the low energy of the LUMO and the consequentially small energy difference between Si–C  $\sigma$ -bonds and the LUMO.

<sup>1</sup>H and <sup>13</sup>C NMR data obtained for cations **1** and **12a** are in general unremarkable. The <sup>1</sup>H and <sup>13</sup>C NMR data obtained for the Tipp-substituted cations **1e**, **6**, and **13** reveal, however, clear indications for multicenter bonding between the positively charged central atom and the *ortho*-CH groups of the Tipp substituent (Table 3 and Figure S11, SI). In particular, the <sup>1</sup>H NMR resonance of the *ortho* methine protons are high field shifted by  $\Delta\delta^1\text{H} = -1.11$  to  $-1.37$ , and the *ortho* methine carbon atoms are deshielded by  $\Delta\delta^{13}\text{C} = 8.4$  to  $9.6$  compared to the corresponding reference silanes (see Table 3). Similar significant changes in the <sup>1</sup>H and <sup>13</sup>C NMR chemical shifts were not detected for the *para* isopropyl groups. In addition, the <sup>1</sup>J(*ortho*-CH) coupling constants in cations **1e**, **6**, and **13** are markedly smaller than those detected for the *para* methine groups ( $\Delta^1J_{\text{CH}} = 14$  Hz). Although these effects appear to be relatively small compared to prototypical compounds that exhibit three-center M–H–C bonding,<sup>24–26</sup> the NMR spectroscopic data for **1e**, **6**, and **13** indicate the onset of a multicenter E<sup>+</sup>⋯H–C interaction (E = Si, Ge). While the consequences of these E<sup>+</sup>⋯H–C interactions are clearly detectable by NMR spectroscopy, IR spectroscopic investigation of the borate **6**[B(C<sub>6</sub>F<sub>5</sub>)<sub>4</sub>] reveals no indications for E<sup>+</sup>⋯H–C bonding; in particular no significant bathochromic shift of the C–H stretch vibrations was detected. In the absence of experimental structural data we tested molecular structures of these cations optimized with DFT methods for possible indications of Si<sup>+</sup>⋯H–C interactions (see Figure S5b and SI). The results of the computations predict for all three cations Tipp<sub>3</sub>Si<sup>+</sup>, **1e**, Tipp<sub>2</sub>EtSi<sup>+</sup>, **6**, and Tipp<sub>2</sub>MeGe<sup>+</sup>, **13**, separations, *d*(E<sup>+</sup>HC), between the positively charged central atom and the *ortho* methine hydrogen atoms (*d*(E<sup>+</sup>HC): 253.5–255.3 pm (**1e**); 238.2, 252.0–256.5 pm (**6**); 245.0, 252.8–253.4 pm (**13**)) that are far longer than the sum of the covalent radii of the tetrel atom and the hydrogen atom (SiH, 148 pm; GeH, 153 pm).<sup>27</sup> They are, however, significantly smaller than the sum of the van der Waals radii (SiH, 330 pm; GeH, 331 pm).<sup>28</sup> Interestingly, an analysis of the B3LYP/6-311++G(3df,3pd) wave function based on the quantum theory of atoms in molecules (QTAIM)<sup>29</sup> for silylium ion **1e** predicts no bond paths between the silicon atom and the methine hydrogen atoms of the *ortho*-isopropyl groups despite their relatively

**Table 3.** Selected  $^1\text{H}$  and  $^{13}\text{C}$  NMR Parameters for Tipp-Substituted Silylium ions **1e** and **6**, Related Silanes **2e** and **7**, and Tipp-Substituted Germylium Ion **13** and Related Germane **11b**

NMR parameter <sup>a</sup>	<b>2e</b>	<b>1e</b>	<b>7</b>	<b>6</b>	<b>11b</b>	<b>13</b>
$\delta^{29}\text{Si}$	-36.7	229.8	-28.5	244.7		
$\delta^1\text{H}(\text{CH}^{\text{ortho}})$	3.62	2.31	3.62	2.25	3.25	2.14
$\delta^{13}\text{C}(\text{CH}^{\text{ortho}})$	33.6	43.2	33.6	44.1	33.7	42.1
$^1J(\text{CH}^{\text{ortho}})$	128 Hz	116 Hz	125 Hz	115 Hz	126 Hz	116 Hz
$\delta^1\text{H}(\text{CH}^{\text{para}})$	2.82	2.72	2.82	2.73	2.81	2.73
$\delta^{13}\text{C}(\text{CH}^{\text{para}})$	34.7	35.0	34.7	35.0	34.1	34.9
$^1J(\text{CH}^{\text{para}})$	128 Hz	130 Hz	125 Hz	129 Hz	127 Hz	129 Hz

<sup>a</sup> $\text{C}_6\text{D}_6$ , 305 K.

close spatial proximity. Only for the Si/ $\text{H}^1\text{C}^1$  pair in **6** with the smallest separation (238.2 pm) was an weakly pronounced bond path with a bond critical point (bcp) of low electron density located (see Figure 8). Comparison of the computed

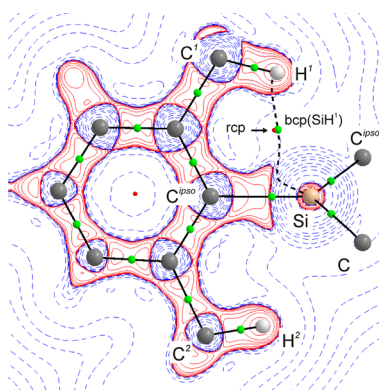


**Figure 8.** Contour plot of the calculated Laplacian of the electron density  $\nabla^2\rho(r)$  of silylium ion **6** in the Si–bcp(SiH<sup>1</sup>)–H<sup>1</sup> plane. Pertinent parts of the molecular graph of cation **6** are projected onto the contour plot. The bond paths that follow the line of maximum electron density between bonded atoms are shown by solid ( $\rho(\text{bcp}) > 0.025 \text{ e bohr}^{-3}$ ) or dashed ( $\rho(\text{bcp}) < 0.025 \text{ e bohr}^{-3}$ ) black lines, and the corresponding bcp's are shown as green, and rcp's as red circles. Red contours indicate regions of local charge accumulation ( $\nabla^2\rho(r) < 0$ ); blue contours indicate regions of local charge depletion ( $\nabla^2\rho(r) > 0$ ).

properties of the charge density at this bcp in **6** with those of SiH bonds of standard compounds such as  $\text{Me}_3\text{SiH}$  (two-electron, two-center (2e-2c) bond) and the  $[\text{Me}_3\text{Si}-\text{H}-\text{CMe}_3]^+$  cation, **15** (2e-3c bond, see Table 4), suggests only small interactions between the central silicon atom and the

**Table 4.** Properties of the Computed Electron Density at the Bond Critical Points of E–H Bonds in Cation **6** and Model Compounds According to QTAIM Analysis (see also Figures Sb and 8)

bond type	compd	$\rho(r)$ [e bohr <sup>-3</sup> ]	$\nabla^2\rho$ [e bohr <sup>-5</sup> ]	atomic distance [pm]
Si–H	$\text{Me}_3\text{Si}-\text{H}$	+0.1206	+0.1496	149.2
	$[\text{Me}_3\text{Si}-\text{H}-\text{CMe}_3]^+$ , <b>15</b>	+0.0536	+0.0322	175.9
	Tipp <sub>2</sub> (Et)Si <sup>+</sup> , <b>6</b> (Si <sup>+</sup> ...H <sup>1</sup> )	+0.0181	+0.0407	238.2
C–H	$\text{Me}_3\text{C}-\text{H}$	+0.2831	-0.9944	109.4
	Tipp <sub>2</sub> (Et)Si <sup>+</sup> , <b>6</b> (C <sup>1</sup> –H <sup>1</sup> )	+0.2696	-0.9006	110.8
	Tipp <sub>2</sub> (Et)Si <sup>+</sup> , <b>6</b> (C <sup>2</sup> –H <sup>2</sup> )	+0.2737	-0.9272	110.3
	$[\text{Me}_3\text{Si}-\text{H}-\text{CMe}_3]^+$ , <b>15</b>	+0.2165	-0.5820	115.9

distant methyl hydrogen atom. In addition the close proximity of the bcp of the SiH<sup>1</sup> bond and the ring critical point (rcp) of the SiC<sup>ipso</sup>C<sup>ortho</sup>C<sup>1</sup>H<sup>1</sup> cycle with nearly identical electron density at rcp and bcp describes a situation near to fissure of that bond (bcp:  $\rho(r) = 0.01815 \text{ e bohr}^{-3}$ , rcp:  $\rho(r) = 0.01813 \text{ e bohr}^{-3}$ ; see Figure 8). Complementary information comes from a comparative analysis of the charge density properties of the C<sup>1</sup>–H<sup>1</sup> bond in cation **6** with those of CH bonds of the standard compounds  $\text{Me}_3\text{CH}$  and cation **15** (see Table 4 and Figure 8). This comparison classifies the C<sup>1</sup>–H<sup>1</sup> bond in cation **6** as a rather regular C–H bond with a calculated electron density at the bcp that is not markedly smaller than that predicted for the C–H bond in  $\text{Me}_3\text{CH}$  (see Table 4). Therefore, the QTAIM analysis provides no resilient indication for significant multiple-center bonding between the *ortho*-CH groups of the Tipp substituent and the central atoms in cations **1e**, **6**, and **13**.<sup>30</sup> This is remarkable in view of the clear NMR spectroscopic evidence for such an interaction. A somewhat related situation was reported recently for  $\text{dmpeTiEtCl}_3$  (dmpe: bis(dimethylphosphino)ethane).<sup>24</sup>

## CONCLUSION

The scope and limitations of the BCS hydride transfer reaction with subsequent substituent exchange of diarylsilylium ions are reported. The major advantage of this procedure is the straightforward and easy synthesis of the starting silanes. In addition, this methodology can also be applied for the synthesis of triarylgemylium ions starting from the appropriate germanes. The here presented results indicate a delicate balance between steric and electronic effects of the starting diarylmethylsilanes and -germanes. In addition essentially non-nucleophilic reaction conditions are necessary for the substituent exchange to take place. In detail, the use of arenes and haloarenes as solvents is mandatory, and weakly coordinating anions such as the borates  $[\text{B}(\text{C}_6\text{F}_5)_4]^-$  and  $[\text{B}_{12}\text{Cl}_{12}]^{2-}$  or carborane monoanions<sup>1e,f</sup> must be applied. Accepting these boundary conditions, the here described variant of the BCS hydride transfer reaction<sup>10</sup> of diarylsilylium ions and -germanes provides an undemanding synthetic route to triarylsilylium and triarylgemylium ions. This opens the field for application of these highly Lewis acidic species in bond activation chemistry and catalysis.<sup>2-5</sup> In addition, the simple generation of these carbocation analogues under essentially stable ion conditions calls for a broader structural investigation of this so far neglected class of compounds. To this end, the solid-state structure of the silylium borate  $[\text{Pemp}_3\text{Si}]_2[\text{B}_{12}\text{Cl}_{12}]$ , **1d**, is presented. The XRD analysis revealed a propeller-shaped triarylsilylium ion with a central tricoordinated silicon atom. In agreement with the obtained solid-state structure, a CP/MAS NMR investigation of

this compound disclosed a highly anisotropic, nearly oblate  $^{29}\text{Si}$  NMR chemical shift tensor, which is characteristic for the local  $C_3$  symmetry of the silylium ion. The close accordance between experimental solid-state  $^{29}\text{Si}$  NMR chemical shift of compound  $[\mathbf{1d}]_2[\text{B}_{12}\text{Cl}_{12}]$  and solution-state  $^{29}\text{Si}$  NMR chemical shift of its  $[\text{B}(\text{C}_6\text{F}_5)_4]^-$  salt indicates that also in arene or haloarene solution the tricoordinated silylium ion structure is preserved. Furthermore, the good agreement between experimental data and the computed  $^{29}\text{Si}$  NMR chemical shift obtained for silylium ion  $\mathbf{1d}$  allows verifying molecular structures of silylium ions obtained by theoretical methods. In this respect it is of interest that NMR investigations of the Tipp-substituted cations  $\mathbf{1e}$ ,  $\mathbf{6}$ , and  $\mathbf{12}$  indicate the onset of a multiple-center bonding between the positively charged group 14 element cation and the *ortho*-methine CH groups of the Tipp substituents. This observation underscores the high electron deficiency of tricoordinated group 14 element cations, and it indicates their high potential in bond activation chemistry.

## EXPERIMENTAL SECTION

**General Procedures.** Diethyl ether and tetrahydrofuran were distilled from sodium/benzophenone. Benzene, toluene,  $[\text{D}_6]$ benzene,  $[\text{D}_8]$ toluene, pentane, and hexane were distilled from sodium. Dichloromethylsilane, bromodurene, bromotriisopropylbenzene, and  $\text{Cs}_2[\text{B}_{12}\text{H}_{12}]$  were purchased from ABCR and used as received. Methylolithium in diethyl ether (1.6 M) and *tert*-butyllithium (1.6 M) in hexane were purchased from Acros Organics and used as received. NMR spectra were recorded on Bruker Avance 500 and Avance III 500 spectrometers at 305 K, if not stated otherwise.  $^1\text{H}$  NMR spectra were calibrated using residual protio signals of the solvent ( $\delta^1\text{H}(\text{CHCl}_3) = 7.24$ ,  $\delta^1\text{H}(\text{C}_6\text{D}_6\text{H}) = 7.20$ ,  $\delta^1\text{H}(\text{CHD}_2\text{CN}) = 1.94$ ).  $^{13}\text{C}$  NMR spectra were calibrated using the solvent signals ( $\delta^{13}\text{C}(\text{CDCl}_3) = 77.0$ ,  $\delta^{13}\text{C}(\text{C}_6\text{D}_6) = 128.0$ ,  $\delta^{13}\text{C}(\text{CD}_3\text{CN}) = 1.32$ ).  $^{29}\text{Si}$  NMR spectra were calibrated against external  $\text{Me}_3\text{HSiCl}$  ( $\delta^{29}\text{Si}(\text{Me}_3\text{SiHCl}) = 11.1$ ),  $^{19}\text{F}$  NMR spectra against external  $\text{CFCl}_3$  ( $\delta^{19}\text{F}(\text{CFCl}_3) = 0.0$ ), and  $^{11}\text{B}$  NMR spectra against  $\text{BF}_3\cdot\text{OEt}_2$  ( $\delta^{11}\text{B}(\text{BF}_3\cdot\text{OEt}_2) = 0.0$ ). High-resolution mass spectra were recorded on a Finnigan MAT 95. IR spectra were recorded on a Bruker Tensor 27. X-ray diffraction analyses were performed on a Bruker Apex II. Structure solution and refinement was done using the SHELXS97 and SHELXL97 software.<sup>31</sup>

All reactions were carried out under inert conditions, using standard Schlenk techniques and argon (5.0), unless stated otherwise.  $[\text{Ph}_3\text{C}][\text{B}(\text{C}_6\text{F}_5)_4]$  was synthesized according to a modified literature procedure.<sup>32</sup> Synthesis and complete spectroscopic data of silanes  $\mathbf{2a,b,d,e}$ ,  $\mathbf{5a}$ , and  $\mathbf{7}$  and  $[\text{B}(\text{C}_6\text{F}_5)_4]^-$  salts of silylium ions  $\mathbf{1a,b,d,e}$  and  $\mathbf{6}$  have been reported previously.<sup>4</sup> Spectroscopic parameters of the  $[\text{B}(\text{C}_6\text{F}_5)_4]^-$  anion have also been reported earlier<sup>4</sup> and are omitted for better overview.

$\text{Cs}_2[\text{B}_{12}\text{Cl}_{12}]$ . This compound was obtained by chlorination of  $\text{Cs}_2[\text{B}_{12}\text{H}_{12}]$  as described by Gu et al.<sup>16d</sup>  $^{11}\text{B}\{^1\text{H}\}$  NMR (160.38 MHz, 298.9 K,  $\text{CD}_3\text{CN}$ ):  $\delta = -13.3$ .

$[\text{Ph}_3\text{C}]_2[\text{B}_{12}\text{Cl}_{12}]$  (modified literature procedure, ref 33). A 10 g amount of  $\text{Cs}_2[\text{B}_{12}\text{Cl}_{12}]$  (12.18 mmol) and 8.04 g of  $[\text{Ph}_3\text{C}][\text{BF}_4]$  (24.35 mmol) were dissolved in 1000 mL of acetonitrile. The dark red solution was stirred overnight, and the solvent subsequently removed under vacuum to yield an orange, amorphous solid. The solid was charged into a Soxhlet extractor and extracted with 1,2-dichloroethane for several hours. When only a colorless solid ( $\text{Cs}[\text{BF}_4]$ ) remained in the Soxhlet filter, the extraction was stopped and the extract stored at  $-15^\circ\text{C}$  for 7 days. A large amount of yellow solid had precipitated, from which the greenish mother liquor was decanted off. The solid was washed once with toluene and twice with pentane. The obtained  $[\text{Ph}_3\text{C}]_2[\text{B}_{12}\text{Cl}_{12}]$  material still contained a large amount of 1,2-dichloroethane according to  $^1\text{H}$  and  $^{13}\text{C}$  NMR spectroscopy. The solvent-free trityl salt could be obtained by drying the product under vacuum for 3 h at  $120^\circ\text{C}$  (65% yield, 16.4 g). Crystals suitable for X-ray diffraction analysis were obtained from an acetonitrile solution at

$-15^\circ\text{C}$ .  $^1\text{H}$  NMR (500.13 MHz, 300 K,  $\text{CD}_3\text{CN}$ ):  $\delta = 7.72$  (d,  $^3J_{\text{HH}} = 8$  Hz, 6H, *o*-H), 7.88 (t,  $^3J_{\text{HH}} = 8$  Hz, 6H, *m*-H), 8.29 (t,  $^3J_{\text{HH}} = 8$  Hz, 3H, *p*-H).  $^{13}\text{C}\{^1\text{H}\}$  NMR (125.70 MHz, 302.8 K,  $\text{CD}_3\text{CN}$ ):  $\delta = 131.3$ , 141.4, 144.2, 213.3 ( $\text{C}^+$ ).  $^{11}\text{B}\{^1\text{H}\}$  NMR (160.46 MHz, 296.9 K,  $\text{CD}_3\text{CN}$ ):  $\delta = -13.3$ .

**2c, Duryl<sub>2</sub>(Me)SiH.** A 5.3 g (46.07 mmol) portion of dichloromethylsilane was added at  $0^\circ\text{C}$  to a Grignard reagent freshly prepared from 19.66 g (92.25 mmol) of bromodurene and 2.25 g (92.55 mmol) of magnesium in 60 mL of THF. The resulting white suspension was allowed to warm to room temperature and stirred overnight. After refluxing for an additional hour, the mixture was poured into an aqueous solution of ammonium chloride. The organic phase was separated, and the aqueous phase extracted three times with pentane. The organic fractions were combined and concentrated, and the resulting colorless residue was recrystallized from ethanol to yield a colorless solid (43%, 6.2 g).  $^1\text{H}$  NMR (499.87 MHz, 305 K,  $\text{CDCl}_3$ ):  $\delta = 0.71$  (d, 3H,  $^3J_{\text{HH}} = 5$  Hz, Si- $\text{CH}_3$ ), 2.17 (s, 12H, *m*- $\text{CH}_3$ ), 2.26 (s, 12H, *o*- $\text{CH}_3$ ), 5.35 (q,  $^3J_{\text{HH}} = 5$  Hz,  $^1J_{\text{SiH}} = 193$  Hz, 1H, Si-H), 6.95 (s, 2H, *p*-H).  $^{13}\text{C}\{^1\text{H}\}$  NMR (125.71 MHz, 305 K,  $\text{CDCl}_3$ ):  $\delta = 1.6$  (Si- $\text{CH}_3$ ), 19.5 (*o*- $\text{CH}_3$ ), 20.5 (*m*- $\text{CH}_3$ ), 131.0, 133.6, 136.5, 139.8.  $^{29}\text{Si}\{^1\text{H}\}$  NMR (99.31 MHz, 305 K,  $\text{CDCl}_3$ ):  $\delta = -32.2$ . HR-MS (EI): calcd 310.2117; found 310.2109. IR (ATR, neat):  $\nu = 2151$  (Si-H)  $\text{cm}^{-1}$ .

**2f, Ph<sub>2</sub>(Me)SiH.** Compound **2f** has been previously reported in the literature,<sup>34</sup> but was prepared analogously to compound **2c**, and purified by distillation under reduced pressure. Bp:  $65\text{--}70^\circ\text{C}/0.1$  mbar (87% yield, 8.7 g).  $^1\text{H}$  NMR (499.87 MHz, 305 K,  $\text{CDCl}_3$ ):  $\delta = 0.79$  (d,  $^3J_{\text{HH}} = 4$  Hz, 3H, Si- $\text{CH}_3$ ), 5.15 (q,  $^3J_{\text{HH}} = 4$  Hz,  $^1J_{\text{SiH}} = 194$  Hz, 1H, Si-H), 7.49–7.53 (m, 6H, Ar-H), 7.72–7.74 (m, 4H, Ar-H).  $^{13}\text{C}\{^1\text{H}\}$  NMR (125.71 MHz, 305 K,  $\text{CDCl}_3$ ):  $\delta = -5.0$  (Si- $\text{CH}_3$ ), 128.0 (*m*-CH), 129.5 (*p*-CH), 134.8 (*o*-CH), 135.3 (*ipso*- $\text{C}^q$ ).  $^{29}\text{Si}\{^1\text{H}\}$  NMR (99.31 MHz, 305 K,  $\text{CDCl}_3$ ):  $\delta = -17.5$ . IR (ATR, neat):  $\nu = 2117$  (Si-H)  $\text{cm}^{-1}$ .

**2g, o-Tol<sub>2</sub>(Me)SiH.** Compound **2g** has been previously reported in the literature,<sup>35</sup> but was prepared in an analogous manner to compound **2c** and purified by distillation under reduced pressure. Bp:  $90^\circ\text{C}/0.2$  mbar (82% yield, 9.4 g).  $^1\text{H}$  NMR (499.87 MHz, 305 K,  $\text{CDCl}_3$ ):  $\delta = 0.88\text{--}0.90$  (m, 3H, Si- $\text{CH}_3$ ), 2.58–2.60 (m, 6H, *o*- $\text{CH}_3$ ), 5.38–5.42 (m,  $^1J_{\text{SiH}} = 193$  Hz, 1H, Si-H), 7.37–7.40 (m, 4H, Ar-H), 7.50–7.53 (m, 2H, Ar-H), 7.69–7.71 (m, 2H, Ar-H).  $^{13}\text{C}\{^1\text{H}\}$  NMR (125.71 MHz, 305 K,  $\text{CDCl}_3$ ):  $\delta = -4.9$  (Si- $\text{CH}_3$ ), 22.5 (*o*- $\text{CH}_3$ ), 125.1, 129.5, 129.8, 134.2, 135.5, 144.1.  $^{29}\text{Si}\{^1\text{H}\}$  NMR (99.31 MHz, 305 K,  $\text{CDCl}_3$ ):  $\delta = -23.6$ . IR (ATR, neat):  $\nu = 2118$  (Si-H)  $\text{cm}^{-1}$ .

**5b, Mes<sub>2</sub>(*i*-Pr)SiH.** An excess (2 equiv) of a freshly prepared isopropylolithium solution in hexane was added dropwise to a solution of 10 g (33.01 mmol) of dimethylchlorosilane in hexane. The resulting mixture was stirred overnight and subsequently refluxed for 2 h. Under intense stirring, 50 mL of deionized water was carefully added and stirring was continued for 1 h. Subsequently, the phases were separated, and the aqueous phase was extracted with hexane twice. The combined organic layers were concentrated and dried under vacuum to yield **5b** as a colorless solid (80%, 8.2 g).  $^1\text{H}$  NMR (499.87 MHz, 305 K,  $\text{CDCl}_3$ ):  $\delta = 1.13$  (d,  $^3J_{\text{HH}} = 7$  Hz, 6H, CH-( $\text{CH}_3$ )<sub>2</sub>), 1.73 (sep,  $^3J_{\text{HH}} = 7$  Hz, 1H, CH-( $\text{CH}_3$ )<sub>2</sub>), 2.25 (s, 6H, *p*- $\text{CH}_3$ ), 2.41 (s, 6H, *o*- $\text{CH}_3$ ), 4.94 (d,  $^3J_{\text{HH}} = 7$  Hz,  $^1J_{\text{SiH}} = 189$  Hz, 1H, Si-H), 6.81 (s, 4H, *m*-CH).  $^{13}\text{C}\{^1\text{H}\}$  NMR (125.71 MHz, 305 K,  $\text{CDCl}_3$ ):  $\delta = 14.3$  (CH-( $\text{CH}_3$ )<sub>2</sub>), 19.9 (*p*- $\text{CH}_3$ ), 21.0 (CH-( $\text{CH}_3$ )<sub>2</sub>), 23.4 (*o*- $\text{CH}_3$ ), 128.8 (*m*-C), 130.4 ( $\text{C}^q$ ), 138.7 ( $\text{C}^q$ ) 144.5 ( $\text{C}^q$ ).  $^{29}\text{Si}\{^1\text{H}\}$  NMR (99.31 MHz, 305 K,  $\text{CDCl}_3$ ):  $\delta = -19.3$ . HR-MS (EI): calcd 310.2117; found 310.2125. IR (ATR, neat):  $\nu = 2164$  (Si-H)  $\text{cm}^{-1}$ .

**5c, Mes<sub>2</sub>(*t*-Bu)SiH.** This compound was prepared in an analogous manner to **5b** and obtained as a colorless solid (98% yield, 10.5 g).  $^1\text{H}$  NMR (499.87 MHz, 305 K,  $\text{CDCl}_3$ ):  $\delta = 1.21$  (s, 9H, C-( $\text{CH}_3$ )<sub>3</sub>), 2.24 (s, 6H, *p*- $\text{CH}_3$ ), 2.41 (s, 6H, *o*- $\text{CH}_3$ ), 4.97 (s,  $^1J_{\text{SiH}} = 190$  Hz, 1H, Si-H), 6.80 (s, 4H, *m*-CH).  $^{13}\text{C}\{^1\text{H}\}$  NMR (125.71 MHz, 305 K,  $\text{CDCl}_3$ ):  $\delta = 20.9$  (C-( $\text{CH}_3$ )<sub>3</sub>), 21.7 (C-( $\text{CH}_3$ )<sub>3</sub>), 24.1 (*o*- $\text{CH}_3$ ), 29.1 (*p*- $\text{CH}_3$ ), 128.8 (*m*-C), 131.4 ( $\text{C}^q$ ), 138.5 ( $\text{C}^q$ ) 144.4 ( $\text{C}^q$ ).  $^{29}\text{Si}\{^1\text{H}\}$  NMR (99.31 MHz, 305 K,  $\text{CDCl}_3$ ):  $\delta = -17.3$ . HR-MS (EI): calcd 324.2273; found 324.2266. IR (ATR, neat):  $\nu = 2163$  (Si-H)  $\text{cm}^{-1}$ .

**5d**,  $Mes_2(Me_3Si)SiH$ . A 0.9 g (129.68 mmol) sample of finely cut lithium was added to a solution of 6 g (19.81 mmol) of chlorodimesitylsilane in 40 mL of THF at 0 °C. The mixture was stirred at that temperature for 5 h. Subsequently, the dark red suspension was separated from excess lithium and 2.15 g (19.79 mmol) of chlorotrimethylsilane was added. The mixture was allowed to warm to room temperature overnight. All volatiles were removed under vacuum, and hexane was added. The suspension was filtrated, and the filtrate was concentrated under vacuum to yield 1,1-dimesityl-2,2,2-trimethylsilane as a colorless solid (87%, 5.87 g).  $^1H$  NMR (500.13 MHz, 298 K,  $CDCl_3$ ):  $\delta$  = 0.22 (s, 9H, Si-( $CH_3$ )<sub>3</sub>), 2.24 (s, 6H, *p*- $CH_3$ ), 2.35 (s, 12H, *o*- $CH_3$ ), 5.04 (s,  $^1J_{SiH}$  = 173 Hz, 1H, Si-H), 6.80 (s, 4H, *m*-CH).  $^{13}C\{^1H\}$  NMR (125.76 MHz, 298 K,  $CDCl_3$ ):  $\delta$  = -0.2 (Si-( $CH_3$ )<sub>3</sub>), 21.0 (*p*- $CH_3$ ), 24.2 (*o*- $CH_3$ ), 128.4 (*m*-C), 130.7 ( $C^q$ ), 138.3 ( $C^q$ ), 144.3 ( $C^q$ ).  $^{29}Si\{^1H\}$  NMR (99.36 MHz, 298 K,  $CDCl_3$ ):  $\delta$  = -53.6 ( $Mes_2HSiSiMe_3$ ), 13.9 ( $Mes_2HSiSiMe_3$ ). HR-MS (EI): calcd 340.2043; found 340.2037. IR (ATR, neat):  $\nu$  = 2138 (Si-H)  $cm^{-1}$ .

**11a**,  $Mes_2(Me)GeH$ . This compound was prepared as described by Castel et al.<sup>36</sup>  $^1H$  NMR (499.87 MHz, 305 K,  $C_6D_6$ ):  $\delta$  = 0.81 (d,  $^3J_{HH}$  = 4 Hz, 3H, Ge- $CH_3$ ), 2.16 (s, 6H, *p*- $CH_3$ ), 2.37 (s, 6H, *o*- $CH_3$ ), 5.58 (q,  $^3J_{HH}$  = 4 Hz, 1H, Ge-H), 6.77 (s, 4H, *m*-CH).  $^{13}C\{^1H\}$  NMR (125.71 MHz, 305 K,  $C_6D_6$ ):  $\delta$  = 1.4 (Ge- $CH_3$ ), 21.0 (*p*- $CH_3$ ), 23.7 (*o*- $CH_3$ ), 129.1 (*m*-C), 134.7 ( $C^q$ ), 138.2 ( $C^q$ ), 143.3 ( $C^q$ ). HR-MS (EI): calcd 328.1246; found 328.1249. IR (ATR, neat):  $\nu$  = 2041 (Ge-H)  $cm^{-1}$ .

**11b**,  $Tipp_2(Me)GeH$ . A freshly prepared Grignard reagent from 17.5 g (61.8 mmol) of bromotriisopropylbenzene and 3.0 g (123.4 mmol) of magnesium in 80 mL of THF was cooled to -60 °C. Then 6.4 g (64.7 mmol) of pure, colorless copper(I) chloride was slowly added through an addition funnel for solids, and the mixture was allowed to warm to room temperature overnight. A 4.7 g (24.2 mmol) amount of methyltrichlorogermane was added, and the mixture was subsequently refluxed for 8 d. After the off-white suspension was cooled to room temperature, 100 mL of 6 M hydrochloric acid was added. After stirring for 10 min the organic layer was separated and the aqueous layer was extracted with diethyl ether twice. All organic fractions were combined, washed with deionized water once, and concentrated under vacuum to give a colorless solid. The solid was dried under vacuum for 3 h and subsequently dissolved in diethyl ether. A 3.5 g (92.2 mmol) portion of  $LiAlH_4$  was added, and the resulting gray suspension was refluxed for 10 h. After the mixture was cooled to room temperature, 100 mL of hydrochloric acid was carefully added dropwise. The mixture was stirred for 1 h, before the phases were separated and the aqueous layer was extracted with diethyl ether twice. All organic layers were combined and concentrated under vacuum to give **11b** as a colorless solid, still containing traces of triisopropylbenzene (53% yield, 6.4 g).  $^1H$  NMR (499.87 MHz, 305 K,  $CDCl_3$ ):  $\delta$  = 0.89 (d,  $^3J_{HH}$  = 4 Hz, 3H, Ge- $CH_3$ ), 1.04 (m, 24H, *o*-CH-( $CH_3$ )<sub>2</sub>), 1.20 (d,  $^3J_{HH}$  = 7 Hz, 12H, *p*-CH-( $CH_3$ )<sub>2</sub>), 2.81 (sep,  $^3J_{HH}$  = 7 Hz, 2H, *p*-CH), 3.25 (sep,  $^3J_{HH}$  = 7 Hz, 4H, *o*-CH), 5.45 (q,  $^3J_{HH}$  = 4 Hz, 1H, Ge-H), 6.92 (s, 4H, *m*-H).  $^{13}C\{^1H\}$  NMR (125.71 MHz, 305 K,  $CDCl_3$ ):  $\delta$  = 2.9 (Ge- $CH_3$ ), 23.9 ( $CH_3$ ), 24.3 ( $CH_3$ ), 24.6 ( $CH_3$ ), 33.7 (*o*-CH-( $CH_3$ )<sub>2</sub>), 34.1 (*p*-CH-( $CH_3$ )<sub>2</sub>), 121.2 (*m*-C), 134.5 ( $C^q$ ), 149.1 ( $C^q$ ), 153.5 ( $C^q$ ). HR-MS (EI): calcd 496.3124; found 496.3117. IR (ATR, neat):  $\nu$  = 2026 (Ge-H)  $cm^{-1}$ .

**Standard Procedure for Preparation of Silylium and Germylium Borates.** In a typical reaction, 500 mg (0.54 mmol) of  $[Ph_3C][B(C_6F_5)_4]$  and, in the case of solid starting material, the corresponding amount of silane or germane (1.6 equiv) were charged into a Schlenk tube and evacuated for 2 h. A 4 mL amount of benzene was added, resulting in a biphasic reaction mixture. In the case of liquid reactants, the silane or germane was added after dissolving the trityl salt via syringe. The resulting mixture was stirred for 1 h, and in the case of Tipp-substituted precursors, for 5 h. After the allotted time, stirring was turned off and the two layers were allowed to separate. The upper layer was removed, and the lower layer washed twice with small portions of benzene. The product was dried under vacuum for 5 min. The triarylsilylium or triarylgermylium borates were isolated as yellow solids.

**1c** $[B(C_6F_5)_4]$ ,  $Duryl_3Si[B(C_6F_5)_4]$ .  $^1H$  NMR (499.87 MHz, 305 K,  $C_6D_6$ ):  $\delta$  = 1.92 (s, 12H, *m*-H), 2.07 (s, 12H, *o*-H), 7.00 (s, 3H, *p*-CH).  $^{13}C\{^1H\}$  NMR (125.71 MHz, 305 K,  $C_6D_6$ ):  $\delta$  = 18.6 (*o*- $CH_3$ ), 21.9 (*p*- $CH_3$ ) 135.8 ( $C^q$ ), 137.5 ( $C^q$ ), 139.4 ( $C^q$ ), 140.6 (*p*-CH).  $^{13}C$  NMR (125.71 MHz, 305 K,  $C_6D_6$ ):  $\delta$  = 18.6 (q,  $^1J_{CH}$  = 126 Hz, *o*- $CH_3$ ), 21.9 (q,  $^1J_{CH}$  = 126 Hz, *p*- $CH_3$ ) 135.8 ( $C^q$ ), 137.5 ( $C^q$ ), 139.4 ( $C^q$ ), 140.6 (dm,  $^1J_{CH}$  = 157 Hz, *p*-CH).  $^{29}Si\{^1H\}$  NMR (99.31 MHz, 305 K,  $C_6D_6$ ):  $\delta$  = 226.5.

**12a** $[B(C_6F_5)_4]$ ,  $Mes_3Ge[B(C_6F_5)_4]$ .  $^1H$  NMR (499.87 MHz, 305 K,  $C_6D_6$ ):  $\delta$  = 1.99 (s, 18H, *o*- $CH_3$ ), 2.08 (s, 9H, *p*- $CH_3$ ), 6.63 (s, 6H, *m*-CH).  $^{13}C\{^1H\}$  NMR (125.71 MHz, 305 K,  $C_6D_6$ ):  $\delta$  = 21.2 (*p*- $CH_3$ ), 23.0 (*o*- $CH_3$ ), 130.0 (C-H), 139.7 ( $C^q$ ), 141.9 ( $C^q$ ), 148.7 ( $C^q$ ).

$Mes_3GeH$ . MS (EI, 70 eV)  $m/z$  (rel intensity in %): 120 (61), 105 (100), 91 (9), 77 (13).

**13** $[B(C_6F_5)_4]$ ,  $Tipp_3MeGe[B(C_6F_5)_4]$ .  $^1H$  NMR (499.87 MHz, 305 K,  $C_6D_6$ ):  $\delta$  = 1.05 (d,  $^3J_{HH}$  = 6 Hz, 24H, *o*-CH-( $CH_3$ )<sub>2</sub>), 1.15 (d,  $^3J_{HH}$  = 6 Hz, 12H, *p*-CH-( $CH_3$ )<sub>2</sub>), 1.51 (s, 3H, Ge- $CH_3$ ), 2.14 (sep,  $^3J_{HH}$  = 6 Hz, 4H, *o*-CH-( $CH_3$ )<sub>2</sub>), 2.73 (sep,  $^3J_{HH}$  = 6 Hz, 2H, *p*-CH-( $CH_3$ )<sub>2</sub>), 7.05 (s, 4H, *m*-CH).  $^{13}C\{^1H\}$  NMR (125.71 MHz, 305 K,  $C_6D_6$ ):  $\delta$  = 20.8 (Ge- $CH_3$ ), 23.2 (*p*-CH-( $CH_3$ )<sub>2</sub>), 24.3 (*o*-CH-( $CH_3$ )<sub>2</sub>), 34.9 (*p*- $CH_3$ ), 42.1 (*o*- $CH_3$ ), 124.0 (*m*-CH), 136.1 ( $C^q$ ), 153.0 ( $C^q$ ), 158.8 ( $C^q$ ).

**1d** $[B_{12}Cl_{12}]$ ,  $[Pemp_3Si]_2[B_{12}Cl_{12}]$ . In a typical reaction, 82 mg (0.079 mmol, 1.0 equiv) of  $[Ph_3C]_2[B_{12}Cl_{12}]$  and 80 mg (0.167 mmol, 2.15 equiv) of silane **2d** were charged into a Schlenk tube and evacuated for 2 h. A 4 mL portion of *ortho*-dichlorobenzene was added and gave a yellow suspension, which darkened slowly. After approximately 1 h the mixture had changed into a yellow solution. To remove marginally undissolved components, the mixture was filtrated using a filter funnel (pore size 4). The solvent can be removed under vacuum to yield pure **1d** $[B_{12}Cl_{12}]$  as a yellow solid. Crystals suitable for single-crystal X-ray diffraction analysis were obtained from the *ortho*-dichlorobenzene solution after four weeks at -15 °C.

**10** $[B(C_6F_5)_4]$ ,  $Mes_2(Me)Si/NCCH_3[B(C_6F_5)_4]$ . A 500 mg (0.54 mmol) amount of  $[Ph_3C][B(C_6F_5)_4]$  and 154 mg (0.55 mmol) of silane were charged into a Schlenk tube and evacuated for 2 h. A 2 mL sample of acetonitrile was added, and the resulting mixture was stirred for 1 h. All volatiles were evaporated, and 3 mL of benzene was added, resulting in a two-phase reaction mixture. The upper phase was removed, and the lower phase washed twice with small portions of benzene. The product was dried under vacuum and obtained as a colorless solid.  $^1H$  NMR (499.87 MHz, 305 K,  $C_6D_6$ ):  $\delta$  = 0.81 (s, 3H, Si- $CH_3$ ), 1.08 (s, 3H, NC- $CH_3$ ), 2.05 (s, 12H, *o*- $CH_3$ ), 2.13 (s, 6H, *p*- $CH_3$ ), 6.72 (s, 4H, *m*-H).  $^{13}C\{^1H\}$  NMR (125.71 MHz, 305 K,  $C_6D_6$ ):  $\delta$  = 0.3 (Si- $CH_3$ ), 4.5 (NC- $CH_3$ ), 20.7 (*p*- $CH_3$ ), 23.3 (*o*- $CH_3$ ), 123.1, 128.5, 130.8, 143.6, 143.7.  $^{29}Si\{^1H\}$  NMR (99.31 MHz, 305 K,  $C_6D_6$ ):  $\delta$  = 10.6.

$Mes_3GeH$  by Derivation of **12a** $[B(C_6F_5)_4]$ . A 197 mg (0.68 mmol) amount of *n*-Bu<sub>3</sub>SnH was slowly added via a Hamilton syringe to a well-stirred biphasic reaction mixture of 832 mg (0.75 mmol) of **12a** $[B(C_6F_5)_4]$  in benzene. During the addition the dark color of the reaction mixture lightened. After completed addition, stirring was stopped and the phases were allowed to separate. The top layer, containing the neutral germane, was separated via PTFE cannula, the solvent was evaporated, and the colorless solid residue was analyzed by GC/MS and NMR spectroscopy.  $^1H$  NMR ( $CDCl_3$ , 499.87 MHz, 305 K):  $\delta$  = 2.15 (s, 18H, *o*- $CH_3$ ), 2.25 (s, 9H, *p*- $CH_3$ ), 5.85 (s, 1H, GeH), 6.79 (s, 6H, *m*-CH).  $^{13}C\{^1H\}$  NMR ( $CDCl_3$ , 125.69 MHz, 305 K):  $\delta$  = 21.0 (s, *p*- $CH_3$ ), 23.6 (s, *o*- $CH_3$ ), 128.8 (s, *m*-CH), 134.9 (s, *p*- $C^q$ ), 138.2 (s, *o*- $C^q$ ), 143.6 (s, *ipso*- $C^q$ ). IR (ATR, neat):  $\nu$  [ $cm^{-1}$ ] 2031 (m, Ge-H). MS (EI, 70 eV)  $m/z$  (rel intensity in %): 431 (1), 312 (30), 192 (100), 119 (36), 105 (83), 91 (30), 77 (18).

## ■ ASSOCIATED CONTENT

### Supporting Information

Relevant NMR spectra, X-ray crystallographic information for compounds **1d** $[B(C_6F_5)_4]$ , **2d**, and  $[Ph_3C]_2[B_{12}Cl_{12}]$ ; details of the solid-state NMR measurements and all computational details including a table of absolute energies and Cartesian

coordinates of pertinent molecular structures. This material is available free of charge via the Internet at <http://pubs.acs.org>.

## AUTHOR INFORMATION

### Corresponding Author

\*E-mail: [thomas.mueller@uni-oldenburg.de](mailto:thomas.mueller@uni-oldenburg.de).

### Notes

The authors declare no competing financial interest.

## ACKNOWLEDGMENTS

This work is dedicated to Prof. Werner Uhl on occasion of his 60th birthday. This study was supported by the CvO University Oldenburg and by the DFG (Mu-1440/7-1). The High End Computing Resource Oldenburg (HERO) at the CvO University is thanked for computer time.

## REFERENCES

- (1) Reviews: (a) Lee, V. Y.; Sekiguchi, A. *Organometallic Compounds of Low-Coordinate Si, Ge, Sn and Pb*; Wiley: Chichester, 2010. (b) Lee, V. Y.; Sekiguchi, A. *Acc. Chem. Res.* **2007**, *40*, 410. (c) Kochina, T. A.; Vrazhnov, D. V.; Sinotova, E. N.; Voronkov, M. G. *Russ. Chem. Rev.* **2006**, *75*, 95. (d) Müller, T. *Adv. Organomet. Chem.* **2005**, *53*, 155. (e) Reed, C. A. *Chem. Commun.* **2005**, 1669. (f) Reed, C. A. *Acc. Chem. Res.* **1998**, *31*, 133.
- (2) (a) Klare, H. F. T.; Oestreich, M. *Dalton Trans.* **2010**, 39, 9176–9184. (b) Meier, G.; Braun, T. *Angew. Chem., Int. Ed.* **2009**, *48*, 1546–1548. (c) Schulz, A.; Villinger, A. *Angew. Chem., Int. Ed.* **2012**, *51*, 4526–4528. (d) Schmidt, R. K.; Mütter, K.; Mück-Lichtenfeld, C.; Grimme, S.; Oestreich, M. *J. Am. Chem. Soc.* **2012**, *134*, 4421.
- (3) C–F activation: (a) Douvris, C.; Ozerov, O. V. *Science* **2008**, *321*, 1188. (b) Scott, V. J.; Çelenligil-Çetin, R.; Ozerov, O. V. *J. Am. Chem. Soc.* **2005**, *127*, 2852. (c) Gu, W.; Haneline, M. R.; Douvris, C.; Ozerov, O. V. *J. Am. Chem. Soc.* **2009**, *131*, 11203. (d) Douvris, C.; Nagaraja, C. M.; Chen, C.-H.; Foxman, B. M.; Ozerov, O. V. *J. Am. Chem. Soc.* **2010**, *132*, 4946. (e) Panisch, R.; Bolte, M.; Müller, T. *J. Am. Chem. Soc.* **2006**, *128*, 9676. (f) Lühmann, N.; Panisch, R.; Müller, T. *Appl. Organomet. Chem.* **2010**, *24*, 533. (g) Lühmann, N.; Hirao, H.; Shaik, S.; Müller, T. *Organometallics* **2011**, *30*, 4087. (h) Duttwyler, S.; Douvris, C.; Fackler, N. L. P.; Tham, F. S.; Reed, C. A.; Baldrige, K. K.; Siegel, J. S. *Angew. Chem., Int. Ed.* **2010**, *49*, 7519. (i) Alleman, O.; Duttwyler, S.; Romanato, P.; Baldrige, K. K.; Siegel, J. S. *Science* **2011**, *332*, 574. (j) Stahl, T.; Klare, H. F. T.; Oestreich, M. *J. Am. Chem. Soc.* **2013**, *135*, 1248.
- (4) Dihydrogen activation: Schäfer, A.; Reissmann, M.; Schäfer, A.; Saak, W.; Haase, D.; Müller, T. *Angew. Chem., Int. Ed.* **2011**, *50*, 12636.
- (5) CO<sub>2</sub> activation: Schäfer, A.; Saak, W.; Haase, D.; Müller, T. *Angew. Chem., Int. Ed.* **2012**, *51*, 2981.
- (6) Model systems for tuneable silyl Lewis acids based on these considerations have been recently suggested: (a) Duttwyler, S.; Do, Q.-Q.; Linden, A.; Baldrige, K. K.; Siegel, J. S. *Angew. Chem., Int. Ed.* **2008**, *47*, 1719. (b) Müller, T. In *Organosilicon Chemistry V*; Auner, N.; Weis, J., Eds.; Wiley-VCH: Weinheim, 2003; p 34.
- (7) (a) Lambert, J. B.; Zhao, Y. *Angew. Chem., Int. Ed.* **1997**, *36*, 400. (b) Lambert, J. B.; Zhao, Y.; Wu, H.; Tse, W. C.; Kuhlmann, B. *J. Am. Chem. Soc.* **1999**, *121*, 5001. (c) Kim, K.-C.; Reed, C. A.; Elliott, D. W.; Mueller, L. J.; Tham, F.; Lin, L.; Lambert, J. B. *Science* **2002**, *297*, 825. (d) Lambert, J. B.; Lin, L. *J. Org. Chem.* **2001**, *66*, 8537.
- (8) (a) Sekiguchi, A.; Matsuno, T.; Ichinohe, M. *J. Am. Chem. Soc.* **2000**, *122*, 11250. (b) Ichinohe, M.; Igarashi, M.; Sanuki, K.; Sekiguchi, A. *J. Am. Chem. Soc.* **2005**, *127*, 9978. (c) Igarashi, M.; Ichinohe, M.; Sekiguchi, A. *J. Am. Chem. Soc.* **2007**, *129*, 12660.
- (9) (a) Ishida, S.; Nishinaga, T.; West, R.; Komatsu, K. *Chem. Commun.* **2005**, 778. (b) Schäfer, A.; Schäfer, A.; Müller, T. *Dalton Trans.* **2010**, 39, 9296.
- (10) (a) Bartlett, P. D.; Condon, F. E.; Schneider, A. *J. Am. Chem. Soc.* **1944**, *66*, 1531. (b) Corey, J. Y. *J. Am. Chem. Soc.* **1975**, *97*, 3237.
- (11) Lambert, J. B.; Zhang, S.; Ciro, S. M. *Organometallics* **1994**, *13*, 2430.
- (12) The Gaussian 03, Rev D.02 version of the program was used.
- (13) See the Supporting Information for further details.
- (14) (a) Müller, T.; Bauch, C.; Ostermeier, M.; Bolte, M.; Auner, N. *J. Am. Chem. Soc.* **2003**, *125*, 2158. (b) Ichinohe, M.; Fukui, H.; Sekiguchi, A. *Chem. Lett.* **2000**, 600.
- (15) Germylium salts reported previously: (a) Sekiguchi, A.; Tsukamoto, M.; Ichinohe, M. *Science* **1997**, *275*, 60. (b) Sekiguchi, A.; Fukawa, T.; Lee, V. Ya.; Nakamoto, M.; Ichinohe, M. *Angew. Chem., Int. Ed.* **2003**, *42*, 1143. (c) Schenk, C.; Drost, C.; Schnepf, A. *Dalton Trans.* **2009**, 773.
- (16) (a) Kessler, M.; Knapp, C.; Sagawe, V.; Scherer, H.; Uzun, R. *Inorg. Chem.* **2010**, *49*, 5223. (b) Avelar, A.; Tham, F. S.; Reed, C. A. *Angew. Chem., Int. Ed.* **2009**, *48*, 3491. (c) Mütter, K.; Fröhlich, R.; Mück-Lichtenfeld, C.; Grimme, S.; Oestreich, M. *J. Am. Chem. Soc.* **2011**, *133*, 12442. (d) Gu, W.; Ozerov, O. V. *Inorg. Chem.* **2011**, *50*, 2726.
- (17) These results also imply a prolate <sup>29</sup>Si shielding tensor ( $\sigma_{11} = \sigma_{22} < \sigma_{33}$ ).
- (18) (a) Herzfeld, J.; Berger, A. E. *J. Chem. Phys.* **1980**, *73*, 6021. (b) Mason, J. *Solid State Nucl. Magn. Reson.* **1993**, *2*, 285.
- (19) Takeuchi, Y.; Takayama, T. In *The Chemistry of Organosilicon Compounds*; Rappoport, Z.; Apeloig, Y., Eds.; Wiley: New York, 1998; Vol. 2, p 267.
- (20) West, R.; Cavalieri, J.; Buffy, J. J.; Fry, C.; Zilm, K. W.; Duchamp, J.; Kira, M.; Iwamoto, T.; Müller, T.; Apeloig, Y. *J. Am. Chem. Soc.* **1997**, *119*, 4972.
- (21) (a) West, R.; Buffy, J. J.; Haaf, M.; Müller, T.; Gehrhuss, B.; Lappert, M. F.; Apeloig, Y. *J. Am. Chem. Soc.* **1998**, *120*, 1639. (b) Müller, T. *J. Organomet. Chem.* **2003**, *686*, 251.
- (22) For an overview on theory of NMR shielding, see: Atkins, P. W.; Friedman, R. S. In *Molecular Quantum Mechanics*, 3rd ed.; Oxford University Press: New York, 1997; p 427.
- (23) Ramsey, N. F. *Phys. Rev.* **1950**, *78*, 699.
- (24) Brookhart, M.; Green, M. H. L. *J. Organomet. Chem.* **1983**, *250*, 395.
- (25) Scherer, W.; McGrady, G. S. *Angew. Chem., Int. Ed.* **2004**, *43*, 1782.
- (26) Lein, M. *Coord. Chem. Rev.* **2009**, *253*, 625.
- (27) Pykkö, M.; Atsumi, M. *Chem.—Eur. J.* **2009**, *15*, 186.
- (28) Mantina, M.; Chamberlin, A. C.; Valero, R.; Cramer, C. J.; Truhlar, D. G. *J. Phys. Chem.* **2009**, *113*, 5806.
- (29) (a) Bader, R. F. W. *Atoms in Molecules: A Quantum Theory*; Clarendon Press: Oxford, 1990. (b) The QTAIM analysis was performed with the AIMALL program. AIMAll (Version 11.05.16); Todd A. Keith, 2011.
- (30) For a summary of AIM criteria that should be fulfilled for C–H...M multiple-center bonding see: Popelier, P. L. A.; Logothetis, G. *J. Organomet. Chem.* **1998**, *555*, 101.
- (31) Sheldrick, G. M. *Acta Crystallogr. A* **2008**, *64*, 112.
- (32) (a) Massey, A. G.; Park, A., J. *J. Organomet. Chem.* **1964**, 245. (b) Chien, J. C. W.; Tsai, W.-M.; Rausch, M. D. *J. Am. Chem. Soc.* **1991**, *113*, 8570.
- (33) Geis, V.; Guttsche, K.; Knapp, C.; Scherer, H.; Uzun, R. *Dalton Trans.* **2009**, 15, 2687.
- (34) Benkeser, R. A.; Foster, D. J. *J. Am. Chem. Soc.* **1952**, *74*, 5314.
- (35) Hernández, D.; Mose, R.; Skrydstrup, T. *Org. Lett.* **2011**, *13*, 732.
- (36) Castel, A.; Riviere, P.; Satgé, J.; Ko, H. *J. Organometallics* **1990**, *9*, 205.